Disorder and Polymorphism in Tetramethylammonium Metaperiodate†

Ross I. Wagner,‡ Robert Bau,‡ Robert Z. Gnann,‡ Paul F. Jones,§ and Karl O. Christe*,‡,||

Loker Hydrocarbon Research Institute and Department of Chemistry, University of Southern California, Los Angeles, California 90089-1661, and Hughes STX, Phillips Laboratory, Propulsion Directorate, Edwards Air Force Base, California 93524

Received December 20, 1996⊗

An improved synthesis is reported for $N(CH_3)_4^+IO_4^-$, and its structure, low-temperature phase transition, polymorphism, and rotational disorder were studied by vibrational spectroscopy, differential scanning calorimetry, and single crystal X-ray diffraction. Its room-temperature structure (phase II) is isomorphic with $N(CH_3)_4ClO_4$ and $N(CH_3)_4BF_4$ and belongs to the tetragonal space group *P*4/*nmm* with $Z = 2$ and unit cell dimensions $a = 8.749(2)$ and $c = 6.054(2)$ Å. The structure was determined with higher precision ($R = 0.036$) than those of $N(CH_3)_4ClO_4$ ($R = 0.134$) and $N(CH_3)_4BF_4$ ($R = 0.089$) and consists of ordered $N(CH_3)_4^+$ cations and disordered IO_4^- anions which undergo free rotation about one of the I−O bonds and thereby satisfy the space group requirement for a 4-fold axis at their special ($^1/_4$, $^1/_4$, *z*) sites. As shown by its variable-temperature Raman spectra, polycrystallinic $N(CH_3)_4IO_4$ undergoes a phase change between +10 and −10 °C. This phase II-phase III transition is of low energy and very broad and could not be detected by DSC. The crystal structure of phase III was determined at −30 °C (orthorhombic, *Pbcm*, Z = 4, $a = 5.969(2)$ Å, $b = 12.214(3)$, $c = 12.447(2)$ Å, $R = 0.038$) and is characterized by ordered $N(CH_3)_4^+$ cations and ordered IO_4^- anions; i.e., the phase II−phase III transition involves the freezing out of the IO_4^- ion rotation. The vibrational spectra of phases II and III were recorded and subjected to factor group analyses. The expected high-temperature, phase II−phase I transition, presumably due to the onset of rotational disorder of the cations and found for $N(CH_3)_4BF_4$ at 328 °C and $N(CH_3)_4ClO_4$ at 340 °C, could not be observed for $N(CH_3)_4IO_4$ because the latter compound explodes violently at about 247 °C before reaching this transition. The results of this study confirm the interpretation, proposed in 1930 by Pauling and repeatedly challenged since then, that the phase transitions in these compounds are due to the onset of ion rotation rather than positional disorder of the rotational oscillation axes.

Introduction

Tetramethylammonium perhalogenates are fascinating compounds. They are highly energetic materials containing a combination of an organic cation with a strongly oxidizing anion. Furthermore, they are of significant interest from a structural point of view. By analogy with ammonium halides, ammonium perhalogenates, and ammonium complex fluoro anion salts, they exhibit phase transitions[1,2] whose rationalization has been a long lasting and much studied challenge to chemists, dating back as far as Linus Pauling in 1930. With his typical grasp for difficult chemical problems, he proposed that the phase transitions in these compounds are due to the onset of ion rotation.[3] In subsequent years, this view has been challenged and alternate interpretations involving the distribution of rotational oscillation axes over a fixed set of possible positions have been proposed.[4] Another interesting problem presented by the tetramethylammonium perhalogenates deals with the general difficulty of packing two sets of tetrahedral ions.[5]

Whereas the lighter homologue, $N(CH_3)_4ClO_4$,[2,4,6,7] is relatively well-known, only very little is known about $N(CH_3)_4IO_4$. It was first reported in 1962, and on the basis of room-temperature Weisenberg photographs, the tetragonal space group *P*4/*ncc* with $Z = 4$, $a = 8.77(2)$ Å, and $c = 12.07(3)$ Å was proposed.[8] A decade later, in a brief note, its X-ray powder diffraction pattern was published and it was suggested that $N(CH_3)_4IO_4$ and $N(CH_3)_4ClO_4$ are isostructural,[9] i.e., belong to the tetragonal space group *P*4/*nmm* with $a = 8.439$ and $c = 6.108$Å for the IO_4^- salt. The only other paper on $N(CH_3)_4IO_4$ which we found in the literature deals with its iodine-127 NQR spectrum.[10]

Experimental Section

Caution! *Tetramethylammonium metaperiodate is about twice as sensitive (35 kg·cm) to impact as cyclotetramethylenetetranitramine (HMX) and also explodes violently when heated at about 247 °C.*

Materials and Methods. All reagents were commercially available high-purity substances (Aldrich) and were used without further purification. Infrared spectra were obtained by using dry powders pressed as either KBr or AgBr pellets in an Econo press (Barnes Engineering Co.) and either a Perkin-Elmer Model 283 or a MIDAC FTIR spectrometer. Raman spectra were recorded on a Cary Model 83 spectrometer using the 488-nm exciting line of an Ar ion laser and a grating premonochromator for the elimination of plasma lines. A Harney−Miller type device was used for recording the low-temperature spectra.[11] The DSC data were recorded using a DuPont Model 910 DSC with a TA

† Dedicated to the memory of Dr. Larry Pugh and Otto Heiney, two former Rocketdyne colleagues and friends who lost their lives in a tragic accident on July 26, 1994.

‡ University of Southern California.

§ Propulsion Directorate, Edwards, AFB.

|| Hughes STX.

⊗ Abstract published in *Advance ACS Abstracts,* May 1, 1997.

(1) Giuseppetti, G.; Mazzi, F.; Tadini, C.; Ferloni, P.; Torre, S. *Z. Krist.* **1992**, *202*, 81 and references cited therein.
(2) Mylrajan, M.; Srinivasan, T. K. K. *J. Raman Spectrosc*. **1991**, *22*, 53 and references cited therein.
(3) Pauling, L. *Phys. Rev.* **1930**, *36*, 430.
(4) Stammler, M.; Bruenner, R.; Schmidt, W.; Orcutt, D. *Adv. X-ray Anal.* **1966**, *9*, 170 and references cited therein.
(5) See for example: Christe, K. O.; Lind, M. D.; Thorup, N.; Russell, D. R.; Fawcett, J.; Bau, R. *Inorg. Chem.* **1988**, *27*, 2450.
(6) Kabisch, G. *J. Raman Spectrosc.* **1980**, *9*, 279.
(7) McCullogh, J. D. *Acta Crystallogr.* **1964**, *17*, 1067.
(8) Ferrari, A.; Braibanti, A.; Tiripicchio, A. *Gazz. Chim. Ital.* **1962**, *92*, 22.
(9) Okrasinski, S.; Mitra, G. *J. Inorg. Nucl. Chem.* **1975**, *37*, 1315.
(10) Burkert, P. K.; Hutter, F. M. *Z. Naturforsch.* **1977**, *32b*, 15.
(11) Miller, F. A.; Harney, B. M. *Appl. Spectrosc.* **1970**, *24*, 271.

S0020-1669(96)01514-5 CCC: $14.00

Table 1. Crystallographic Data for Phases II and III of $N(CH_3)_4IO_4$

	phase II (25 °C)	phase III (−30 °C)
formula	$C_4H_{12}INO_4$	
fw	265.0	
space group	*P*4/*nmm* (No. 129)	*Pbcm* (No. 57)
unit cell dimens, Å	$a = 8.749(2)$	$a = 5.969(2)$
	$c = 6.054(2)$	$b = 12.214(3)$
		$c = 12.447(2)$
V, Å^3	463.4(2)	907.5(4)
Z	2	4
ρ_{calcd}, g cm^{-3}	1.899	1.940
abs coeff (μ), cm^{-1}	34.24	34.97
λ, Å	0.710 73	
R^a	0.036	0.038
$R_w{}^b$	0.038	0.039

$^a R = \sum||F_o| - |F_c||/|F_o|$. $^b R_w = [\sum w(|F_o| = |F_c|)^2/\sum w|F_o|^2]^{1/2}$.

Instruments cooling accessory and DuPont LNCA II liquid N_2 boil off cooler. A DuPont Model 2000 thermal analyst was used for recording and analyzing the data. The samples were crimp sealed in aluminum pans and cooled from 25 to −150 °C at a rate of 3 °C/min, held at −150 °C for 10 min, and then warmed at the same rate back to 25 °C. This cycle was repeated two more times.

Preparation of $N(CH_3)_4IO_4$. To a solution of 4.6067 g (20.21 mmol) of H_5IO_6 in 10 mL of water was added 7.2422 g of a 75% aqueous solution of $(CH_3)_4NOH$ (19.86 mmol). The colorless crystalline product which formed on mixing was recrystallized from H_2O by warming to 75 °C and slowly cooling to 0 °C. The crystals were filtered off and quickly washed with 6 mL of ice water. The solid was dried for 12 h at 25 °C in a dynamic vacuum of 10^{-4} Torr to yield 4.1839 g of $N(CH_3)_4IO_4$ (15.78 mmol = 79.5% yield based on $(CH_3)_4NOH$). The mother liquor and washings were concentrated at room temperature, followed by a similar recrystallization to give an additional 0.8021 g of $N(CH_3)_4IO_4$ (3.03 mmol) for a total recovered yield of 94.7%.

Crystal Structure Determination. Single crystals of $N(CH_3)_4IO_4$ were obtained by recrystallization from H_2O. A suitable crystal having dimensions of 0.35 × 0.35 × 0.45 mm was selected under the microscope and glued to the tip of a glass fiber. The data were collected on a Siemens P4 diffractometer at 25 and −30 °C, and the structures were solved and refined to agreement factors of $R = 0.036$ and 0.038 for 256 and 512 $I > 4\sigma(I)$ observed reflections, respectively. The details of the data collections and structure refinements are given in Table 1.

The room-temperature structure, subsequently referred to as "phase II", was found to be tetragonal, space group *P*4/*nmm* (No. 129). The positions of the iodine atoms were obtained readily from a Patterson map and are of 4*mm* (C_{4v}) symmetry. A difference Fourier map immediately revealed the N, C, and axial O(4) atom positions in $\bar{4}2m$ (D_{2d}), *m* (C_s), and 4*mm* (C_{4v}) sites, respectively. The basal plane oxygen atoms, however, presented a significant amount of difficulty. It became clear that the basal plane oxygen electron density could not be adequately modeled by one, two, or three oxygens; in each case, there was a substantial amount of electron density left over. Because of the 4*mm* (C_{4v}) site symmetry of the iodine atom, each basal plane oxygen atom which was introduced resulted in a total of either four or eight symmetry-related equivalent positions depending on whether the oxygens were located on special (*m*) or general positions. The best duplication of the observed electron density was achieved by the introduction of 3 sets of 8-fold disordered, i.e., 24, basal plane oxygen atoms. The resulting ring of oxygen atoms (see Figures 1 and 2) represents in effect a *circularly disordered* band of basal plane electron density with an infinite symmetry axis. The model used is only a device for refinement and not a true depiction of click-stop disorder. The apparent differences in the bond lengths for different sets of disordered basal plane oxygens are artifacts caused by the stepwise introduction of these oxygens during the refinement procedure and, therefore, are physically not meaningful. The only meaningful bond length is their average value of 1.745(42)Å which is in very good agreement with that of 1.759(12)Å observed for the ordered axial oxygen ligand and shows that the bond lengths of all I−O bonds in IO_4^- are identical within the experimental errors. Also, the averaged O_{ax}−I−O_{eq} bond angle of 110.3(10)° is very close to that of 109.5° expected for an ideal tetrahedron and implies that the IO_4^- tetrahedron is not significantly distorted. Finally, a full-matrix least-squares refinement of the structure was carried out with anisotropic temperature factors for iodine and calculated hydrogen positions to give the final *R* factor. When the hydrogen atoms were originally left out of the refinement and introduced at the final stage, the hydrogen positions found from a difference map were identical to the calculated ones.

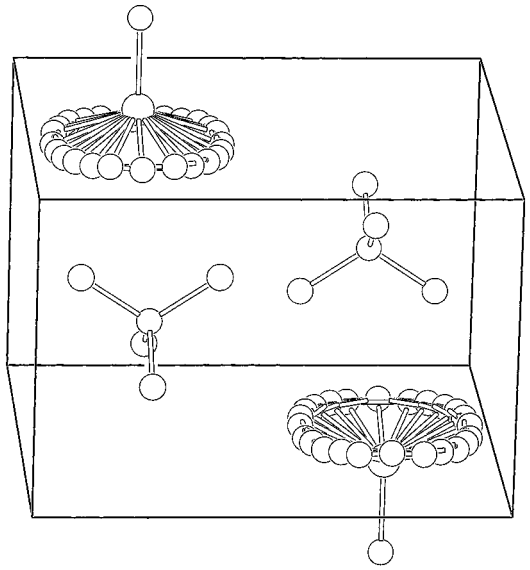

Figure 1. ORTEP drawing of the unit cell of phase II $N(CH_3)_4IO_4$ showing the packing of the ordered $N(CH_3)_4^+$ cations and the 4-fold disordered IO_4^- anions.

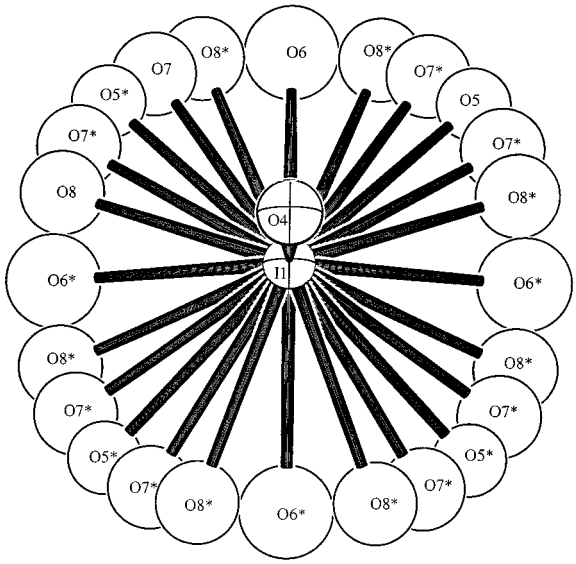

Figure 2. ORTEP drawing of a single disordered IO_4^- anion showing a detailed view of the rotational disorder about one I−O axis with 3 × 8 = 24 oxygen positions located during the refinement process. Atoms O(5) and O(6) are situated on mirror planes and, hence, appear only half as often as O(7) and O(8).

The low-temperature structure, subsequently referred to as "phase III", was determined at −30 °C. Initial attempts to cool crystals to −130 °C met with little success. The X-ray diffraction peaks were badly split, and attempts to anneal these crystals by gradual warming resulted only in minor improvements. A good data set with narrow single peaks was finally obtained at −30 °C for a crystal which had never been cooled before below this temperature.

The symmetry of the diffraction pattern was orthorhombic, with a unit cell volume approximately double that of the tetragonal phase II cell. Systematic extinctions indicated either space group *Pbcm* (No. 57) or $Pbc2_1$, a nonstandard setting of space group $Pca2_1$(No. 29). The structure could be solved by standard heavy atom techniques in either space group, but the former was chosen on the basis of superior interatomic distances and angles. The iodine atom and two oxygen

atoms, O(2) and O(3), are located on a crystallographic mirror plane, while the N atom is situated on a crystallographic 2-fold rotation axis. The structure was refined with anisotropic temperature factors for all non-hydrogen atoms and fixed isotropic factors for the calculated H positions to final agreement factors of $R = 0.038$ and $R_w = 0.039$.

Results and Discussion

Synthesis and Properties of $N(CH_3)_4IO_4$. Pure $N(CH_3)_4IO_4$ can be isolated in high yield from the neutralization of aqueous $N(CH_3)_4OH$ with periodic acid.

$$N(CH_3)_4OH + H_5IO_6 \xrightarrow{H_2O} N(CH_3)_4IO_4 + 3H_2O$$

This simple and rapid procedure provides birefringent, high-purity crystals directly from the reaction mixture. The compound is stable at room temperature but sensitive to impact. It is twice as sensitive (35 kg·cm) as HMX (cyclotetramethylenetetranitramine or octagen). It also explodes violently at about 247 °C before melting and, therefore, should be handled with caution.

Our results are in fair agreement with the previous brief reports on this compound. Ferrari et al. had correctly found that the compound explodes on heating and had given unit cell dimensions in agreement with ours, except for a doubled *c* axis and a slightly different space group, i.e., *P*4/*ncc*.[8] Okrasinski and Mitra had correctly recognized that at room temperature $N(CH_3)_4IO_4$ and $N(CH_3)_4ClO_4$ are isostructural and that the compound explodes at about 220 °C, but their given unit cell dimensions (tetragonal, $a = 8.439$, $c = 6.108$Å) were somewhat inaccurate.[9]

Isomorphism and Phase Transitions of $N(CH_3)_4IO_4$, $N(CH_3)_4ClO_4$, and $N(CH_3)_4BF_4$. As previously suggested by Okrasinski and Mitra[9] and confirmed by crystal structure determinations for $N(CH_3)_4ClO_4$,[7] $N(CH_3)_4BF_4$,[1] and $N(CH_3)_4IO_4$ (see below), these three compounds are isostructural at room temperature. Furthermore, it was shown that these compounds undergo at higher and lower temperatures similar phase transitions.[2,4,12] Therefore, it appears that these compounds are isomorphic and exhibit the following three phases: a high-temperature phase (phase I), a room-temperature phase (phase II), and a low-temperature phase (phase III). Whereas the structure of phase II is known from this and previous[1,7] studies and consists of ordered $N(CH_3)_4^+$ cations and disordered anions, the structure of phase I is unknown and that of phase III will be discussed below.

The high-temperature, phase II−phase I, transition has previously been observed to occur for $N(CH_3)_4ClO_4$ at 340 °C[4] and for $N(CH_3)_4BF_4$ at 328 °C[12] but cannot be observed for $N(CH_3)_4IO_4$ because the compound consistently detonates at about 247 °C before reaching this transition. The low-temperature, phase II−phase III, transition has previously been observed for $N(CH_3)_4BF_4$ at −119 °C by DSC,[12] but the only structural information about phase III is a low-temperature Raman spectrum of $N(CH_3)_4ClO_4$ at −183 °C which indicates freezing out of the anion disorder and an increased number of molecules per unit cell.[2]

For $N(CH_3)_4IO_4$, DSC measurements between −150 and 25 °C did not reveal any observable phase transitions, even at the highest sensitivity levels and with very slow heating and cooling rates, indicating that the low-temperature phase transition, which is evident from the X-ray diffraction and Raman data (see below), is broad and of low energy. Evidence for the broadness and possible hysteresis comes from the Raman data which show a gradual transition from phase II to phase III over a 20 °C temperature range. Evidence for the low energy is based on the small difference of densities between phases II and III from the X-ray data (see Table 1). It should be noted that the previously reported low- and high-temperature phase transitions for $N(CH_3)_4BF_4$ have also been very weak and broad and were barely detectable by DSC.[12] To check the sensitivity of our DSC equipment, the low-temperature phase transition of $N(CH_3)_4BF_4$ was reexamined and was observed as a very weak and broad first-order transition, as previously reported.[12]

Table 2. Atomic Coordinates ($\times 10^4$) and Equivalent Isotropic Displacement Coefficients ($Å^2 \times 10^3$) for Phase II of $N(CH_3)_4IO_4$

	x	*y*	*z*	*U*(eq)[a]	symm[b]
I(1)	2500	2500	9444(2)	52(1)	4*mm*
N(2)	2500	7500	5000	47(2)	42*m*
C(3)	3880(11)	7500	6382(12)	77(2)	*m*
O(4)	2500	2500	12343(16)	78(2)	4*mm*
O(5)	1091(18)	1091(18)	8504(20)	95(2)	*m*
O(6)	2500	770(21)	8390(21)	161(2)	*m*
O(7)	3561(21)	897(21)	8441(21)	125(2)	
O(8)	4200(21)	1798(20)	8460(21)	126(2)	

[a] Equivalent isotropic *U* defined as one-third of the trace of the orthogonalized $\mathbf{U}_{ij}$ tensor. [b] Atomic site symmetry.

Table 3. Bond Lengths[a] (Å) and Bond Angles[a] (deg) for Phase II of $N(CH_3)_4IO_4$

I(1)−O(4)	1.755(9)	I(1)−O(5)	1.833(22)
I(1)−O(6)	1.643(17)	I(1)−O(7)	1.788(18)
I(1)−O(8)	1.716(18)	N(2)−C(3)	1.469(9)
av I(1)−O(5,6,7,8)	1.745(42)		
O(4)−O(1)−O(5)	108.1(4)	O(4)−I(1)−O(6)	112.9(5)
O(4)− I(1)−O(7)	109.9(4)	O(4)−I(1)−O(8)	110.3(4)
O(5)− I(1)−O(8)	103.5(6)	C(3)−N(2)−C(3′)	110.6(6)
C(3)−N(2)−C(3″)	108.9(3)		
av O(4)−I(1)−O(5,6,7,8)	110.3(10)		

[a] Only the average I(1)−O and O(4)−I(1)−O(5,6,7,8) values are physically meaningful. The individual values are artifacts of the refinement.

Crystal Structure of Phase II $N(CH_3)_4IO_4$. The room-temperature (phase II) crystal structure of $N(CH_3)_4IO_4$ was determined and is summarized in Tables 2 and 3 and Figures 1 and 2. As can be seen, the structure consists, in analogy to the known phase II structures of $N(CH_3)_4BF_4$[1] and $N(CH_3)_4ClO_4$,[7] of well-ordered tetrahedral $N(CH_3)_4^+$ cations and disordered IO_4^- anions. As pointed out already above, the different basal plane I−O bond lengths and O(4)−I−O(5−8) bond angles, given in Table 3, are artifacts of the refinement procedure, and their averages of 1.745(42)Å and 110.3(10)°, respectively, are the only physically meaningful values. The average basal plane I−O bond length value of 1.745(42)Å is in good agreement with the axial I−O(4) distance of 1.759(12)Å, which is not influenced by the rotational disorder, and the I−O bond length of 1.775(7)Å observed for IO_4^- in $NaIO_4$.[13] The average O_{ax}−I−O_{eq} bond angle of 110.3(10)° and the similarity of the I−O_{ax} and I−O_{eq} bond lengths demonstrate that the distortion of IO_4^- in phase II $(TMA)IO_4$ from an ideal tetrahedron is insignificant. The circular disorder, found for the basal plane oxygen atoms, suggests essentially free rotation of the IO_4^- tetrahedra about their I−O(4) bonds located along the *c*-axis. The resulting infinite symmetry axis fulfills the 4*mm* site symmetry requirements resulting from their 2c special positions in space group *P*4/*nmm*. The packing diagram, shown in Figure 2, is very simple. The primitive unit cell contains two molecules which are related by an inversion center.

(12) Zabinska, G.; Ferloni, P.; Sanesi, M. *Thermochim. Acta* **1987**, *122*, 87.

(13) Kalman, A.; Cruickshank, D. W. J. *Acta Crystallogr.* **1970**, *B26*, 782.

Table 4. Atomic Coordinates ($\times 10^4$) and Equivalent Isotropic Displacement Coefficients ($Å^2 \times 10^3$) for Phase III of $N(CH_3)_4IO_4$

	x	*y*	*z*	*U*(eq)[a]
I(1)[b]	−553(1)	5113(1)	2500	35(1)
O(2)[b]	2356(11)	5023(6)	2500	53(1)
O(3)[b]	−1317(15)	6486(7)	2500	90(1)
O(4)	−1577(12)	4519(7)	3669(6)	118(1)
N(5)[c]	−5131(12)	2500	5000	32(1)
C(6)	−6558(13)	3285(6)	4386(7)	57(1)
C(7)	−3691(12)	3127(7)	5764(6)	52(1)

[a] Equivalent isotropic *U* defined as one-third of the trace of the orthogonalized $\mathbf{U}_{ij}$ tensor. [b] Atom with population 0.5 and site symmetry *m*. [c] Atom with population 0.5 and site symmetry 2.

Table 5. Bond Lengths (Å) and Bond Angles (deg) for Phase III of $N(CH_3)_4IO_4$

I(1)−O(2)	1.740(7)	I(1)−O(3)	1.738(8)
I(1)−O(4)	1.737(8)	I(1)−O(4′)	1.737(8)
N(5)−C(6)	1.493(9)	N(5)−C(7′)	1.494(8)
N(5)−C(6′)	1.493(9)	N(5)−C(7′)	1.494(8)
O(2)−I(1)−O(3)	108.8(4)	O(2)−I(1)−O(4)	109.0(3)
O(3)−I(1)−O(4)	108.1(3)	O(2)−I(1)−O(4′)	109.0(3)
O(3)−I(1)−O(4′)	108.1(3)	O(4)−I(1)−O(4′)	113.8(5)
C(6)−N(5)−C(7)	109.0(4)	C(6−N(5)−C(6′)	110.4(7)
C(7)−N(5)−C(6′)	109.4(4)	C(6)−N(5)−C(7′)	109.4(4)
C(7)−N(5)−C(7′)	109.7(7)	C(6′)−N(5)−C(7′)	109.0(4)

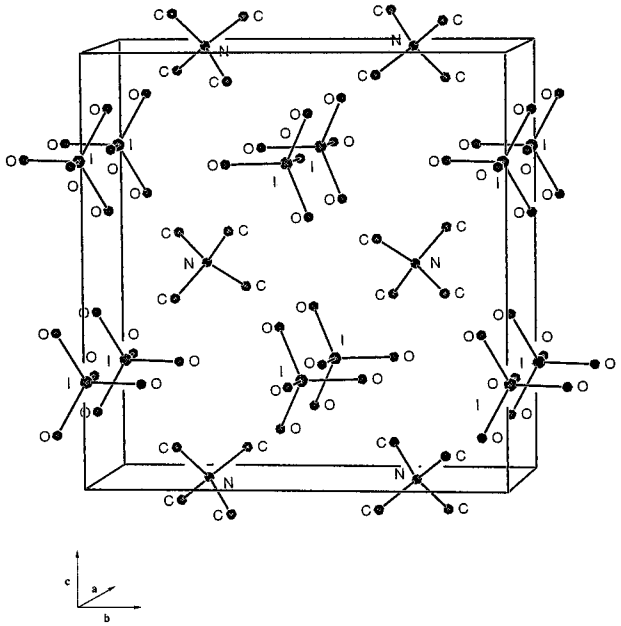

Figure 3. Packing diagram for phase III $N(CH_3)_4IO_4$ viewed along the *a* axis.

Crystal Structure of Phase III $N(CH_3)_4IO_4$. As shown by low-temperature Raman spectroscopy (see below), the rotational disorder of the IO_4^- anions in $N(CH_3)_4IO_4$ is gradually frozen out between +10 and −10 °C. The broadness of this transition and possibly some hysteresis preempted a more precise determination of the transition temperature. The crystal structure of the low-temperature phase (phase III) was determined at −30 °C and is summarized in Tables 4 and 5 and Figures 3 and 4. In phase III, both, the $N(CH_3)_4^+$ cation and IO_4^- anions are ordered and deviate only very little from their ideal tetrahedral geometries. The packing (see Figures 3 and 4) can be derived from a primitive cubic arrangement with the deviations caused by the nonspherical ions. In the direction of the crytallographic *a* axis, the IO_4^- tetrahedra are stacked along their 3-fold and the $N(CH_3)_4^+$ tetrahedra along their 2-fold axes. Along the *b*- and *c*-axes, the IO_4^- stacks alternate with the axial oxygens pointing in one stack to the left and in the other to the right,

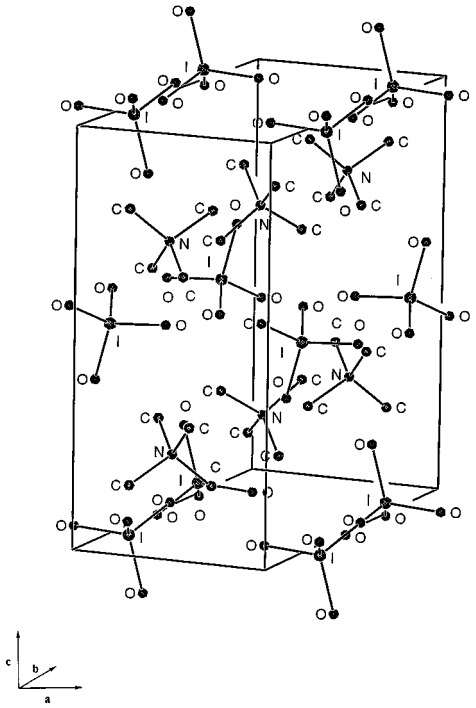

Figure 4. Packing diagram for phase III $N(CH_3)_4IO_4$ viewed along the *b* axis.

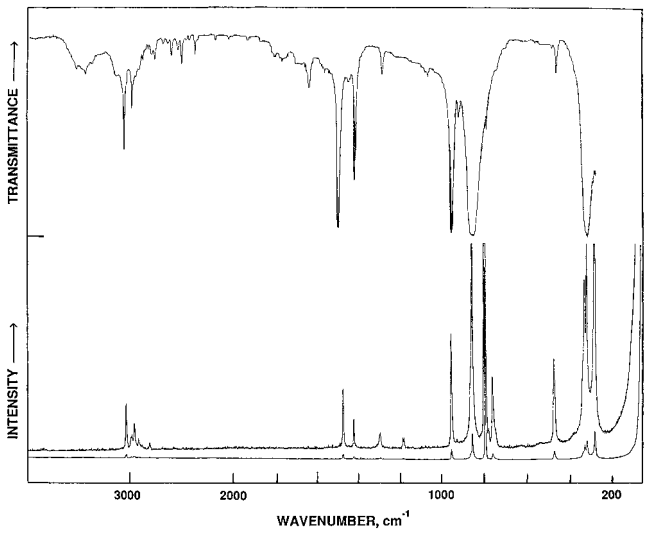

Figure 5. Solid-state infrared and Raman spectra of the tetragonal room-temperature phase of $N(CH_3)_4IO_4$. The Raman spectra were recorded at two different sensitivity settings.

and the orientation of the $N(CH_3)_4^+$ stacks also alternates which causes a doubling of the molecules per unit cell. Along the *b*-axis, the $N(CH_3)_4^+$ cations stack in an interlocking mode with a 90° twist between the ions

and along the *c*-axis, they alternate along a C_{2v} axis as

Vibrational Spectra. The infrared and Raman spectra of the room-temperature phase (phase II) are shown in Figure 5, and the observed frequencies and their assignments are summarized in Table 6. The observed spectra are in good agreement

Table 6. Vibrational Spectra of Phase II and Phase III $N(CH_3)_4IO_4$ and Their Assignments in Point Group T_d

obsd freq, cm^{-1} (rel intensity)			assgnts	
phase II (25 °C)		phase III (−113 °C)		
IR	Ra	Ra	$N(CH_3)_4^+$	IO_4^-
3042 mw	3037 (2.5)	3038 (4)		
		3031 (1.3)		
		3026 (1.2)	$\nu_5(E)$	
			$\nu_{14}(F_2)$	
2970 w	2995 (0.7)	2965 (0+)	$\nu_1(A_1)$	
	2958 (1.5)	2956 (2)	+combin bands	
	2917 (0.5)			
	2882 sh			
	2810 (0.4)	2806 (0.4)		
1635 w				$(\nu_1 + \nu_3)(F_2)$
1490 ms			$\nu_{15}(F_2)$	
	1465 (2.7)	1469 (3)	$\nu_6(E)$	
		1463 (4)	$\nu_2(A_1)$	
1412 m	1413 (1.4)	1412 sh		
		1409 (2)	$\nu_{16}(F_2)$	
1288 w	1287 (0.7)	1287 (1)	$\nu_{17}(F_2)$	
	1177 (0.4)	1181 (0.6)	$\nu_7(E)$	
		1172 (0.4)		
951 s	950 (5.4)	951 (9)	$\nu_{18}(F_2)$	
922 w	919 (0.1)		$2\nu_{19}(F_2)$	
855 sh	858 sh	861 (11)		
847 vs	850 (14)	851 (21)		$\nu_3(F_2)$
	843 sh	843 (8)		
789 vw	791 (100)	790 (100)		$\nu_1(A_1)\ I^{16}O_4^-$
	771 (0.8)	771 (0.8)		$\nu_1(A_1)\ I^{16}O_3{}^{18}O^-$
	755 (3.3)	756 (7)		
	742 sh	749 (1)	$\nu_3(A_1)$	
		738 (0.8)		
	529 (0+)			
462 mw	462 (4.1)	456 (4)	$\nu_{19}(F_2)$	
		370 (0.5)		
	322 sh	327 (13)		
315 sh	317 (7)	319 (5)		$\nu_4(F_2)$
302 s		312 (8)		
297 sh	305 (10)	303 (12)		
		268 (22)		
	266 (14)	264 (18)		$\nu_2(E)$

with the expectations for tetrahedral $N(CH_3)_4^+$ [6,14] and IO_4^- [15] ions. Although the $N(CH_3)_4^+$ cations in phase II $N(CH_3)_4IO_4$ occupy D_{2d} sites which correlate to the factor group D_{4h}, the deviations from tetrahedral symmetry are not large enough to cause significant site group and factor group splittings and, therefore, the assignments were made for T_d symmetry. The assignments for IO_4^- are based on those previously reported for its Na^+, K^+, Rb^+, NH_4^+, Ag^+, Li^+, and Cs^+ salts,[15] and their frequencies are very similar. By analogy with the previously reported IO_4^- salts,[15] the IO_4^- bands of $N(CH_3)_4IO_4$ also exhibit splittings for some of the degenerate modes. The differences in the splitting patterns are due to the fact that $N(CH_3)_4IO_4$ is not isotypic with these other periodates which have scheelite-type structures with IO_4^- occupying S_4 sites, while the IO_4^- ions in $N(CH_3)_4IO_4$ are located on C_{4v} sites and exhibit rotational disorder. Whereas the observed splittings of $\nu_3(F_2)$ and $\nu_4(F_2)$ of IO_4^- can be attributed to a lifting of the degeneracies of these modes, i.e., site group splittings, the very weak satellite band at 770 cm^{-1} observed for $\nu_1(A_1)$ in the Raman spectrum cannot be explained in the same manner. It has the correct intensity (0.8%) and frequency shift (20 cm^{-1}) for $I^{16}O_3{}^{18}O^-$ based on the natural abundance of ^{18}O and, therefore, is assigned to $\nu_1(A_1)$ of $I^{16}O_3{}^{18}O^-$.[2] The observation of $\nu_1(A_1)$ in the infrared spectrum, albeit as a very weak band, is in accord with the C_{4v} site symmetry of IO_4^-. This allows this mode, which is forbidden under T_d symmetry, to become infrared active.

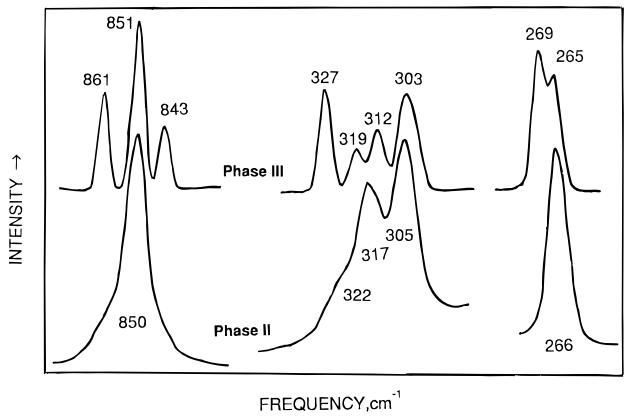

Figure 6. Raman bands of the IO_4^- anion in phase II (25 °C) and phase III (−113 °C) $N(CH_3)_4IO_4$.

The Raman spectrum of phase III $N(CH_3)_4IO_4$ (see Table 6) was recorded at −113 °C and significantly differs from the phase II spectrum. It exhibits pronounced splittings for the E and F_2 modes of IO_4^- (see Figure 6), which is not surprising in view of the IO_4^- ions being well ordered. The four bands observed for $\nu_4(F_2)$ exceed the number of three allowed from site symmetry arguments, and additional factor group splittings must be invoked. Therefore, factor group analyses were carried out for both, IO_4^- and $N(CH_3)_4^+$, ions in phase III $N(CH_3)_4IO_4$, and the results are summarized in Tables 7 and 8. As can be

(14) Christe, K. O.; Dixon, D. A.; Wilson, W. W. *J. Am. Chem. Soc.* **1994**, *116*, 7123 and references cited therein.
(15) Siebert, H.; Wieghardt, G. *Spectrochim. Acta, Part A* **1971**, *27A*, 1677 and references cited therein.

Table 7. Correlations for the IO_4^- Intramolecular Vibrational Modes in Phase III $N(CH_3)_4IO_4$

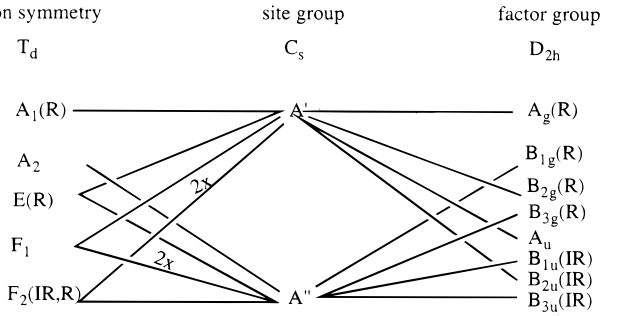

Table 8. Correlations for the $N(CH_3)_4^+$ Intramolecular Vibrational Modes in Phase III $N(CH_3)_4IO_4$

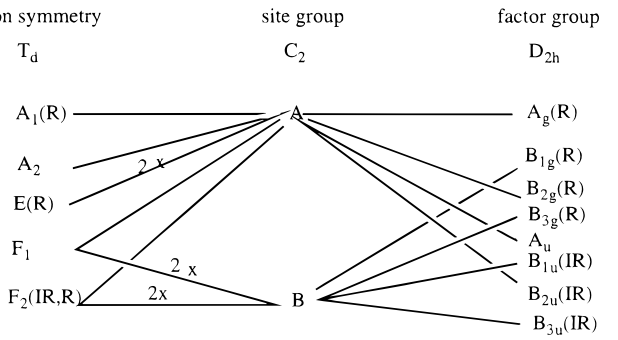

seen from these tables, the extra Raman bands can be readily accounted for by factor group splittings.

In view of the difficulties of observing the phase II−phase III transition by DSC (see above), the pronounced changes in the Raman spectra offer an excellent method to monitor this transition. It was found that the change in the Raman spectra from phase II to phase III was gradual and was spread out over a temperature range of about 20 °C for a polycrystallinic sample of $N(CH_3)_4IO_4$. This is not surprising if one considers the mechanism of this phase change. The results from the X-ray structure determinations for phase II and phase III (see above) establish that the phase change is due to freezing out the free rotation of the IO_4^- ions. This freezing out of the free rotation must involve a gradual slow down of the rotational speed and, for a polycrystallinic sample, might not be a sharp event. For a single crystal, this phase change should be sharp because the unit cell contraction associated with the phase change should stop the free rotation of all ions at once and only allow their oscillation around the rotational axes. In a polycrystallinic sample, the temperature range of this transition could be broadened if the crystal lattice change does not occur simultaneously in all crystals.

The $N(CH_3)_4^+$ part of the Raman spectra also undergoes some changes upon the phase II−phase III transition, probably due to the different site symmetries and factor groups involved. However, the changes in the spectra are not as pronounced as for IO_4^- because the $N(CH_3)_4^+$ cations are ordered in both phases.

Conclusions. The results of this study establish the phase II and phase III structures of $N(CH_3)_4IO_4$ and, thereby, identify the nature of the phase transition. In agreement with Pauling's original proposal,[3] it is shown that the phase change is due to the onset of free ion rotation and is not caused by positional disorder of the rotational oscillation axes.[4] The three phases, typically found for this group of salts composed of tetrahedral ions, can be described in the following manner. Phase III (low-temperature phase): Both the anion and cation are ordered. Phase II (room-temperature phase): The larger ion, usually NR_4^+, is ordered and the smaller counterion is rotationally disordered. Phase I (high temperature phase): Both ions presumably are rotationally disordered.

As expected, the symmetry of the unit cells increases and their specific density decreases with increasing disorder of the ions. The phase transitions involved are generally of low energy and relatively broad.

Acknowledgment. The authors thank Prof. G. A. Olah and Drs. E. J. Wucherer, S. J. Rodgers, W. W. Wilson, and M. Petrie for support and stimulating discussions. The work at the Phillips Laboratory is financially supported by the Propulsion Directorate of the U.S. Air Force, that at USC by the National Science Foundation, and R.Z.G. is grateful to the Deutsche Forschungs Gemeinschaft for a scholarship.

Supporting Information Available: Structure determination summaries (Tables S1 and S4), anisotropic displacement coefficients (Tables S2 and S5), and H atom coordinates and isotropic displacement coefficients (Tables S3 and S6) for phases II and III, respectively, of $N(CH_3)_4IO_4$) (6 pages). Ordering information is given on any current masthead page.

IC961514V